Effect of vehicle velocity on exciting the lateral dynamic response of two-span integral bridges

Prendergast, Luke; Gavin, Kenneth; Hester, David

Publication date
2016

Document Version
Final published version

Published in
Proceedings of Civil Engineering Research in Ireland 2016

Citation (APA)
Prendergast, L., Gavin, K., & Hester, D. (2016). Effect of vehicle velocity on exciting the lateral dynamic response of two-span integral bridges. In *Proceedings of Civil Engineering Research in Ireland 2016: 29th-30th August, Galway, Ireland*

Effect of vehicle velocity on exciting the lateral dynamic response of two-span integral bridges

Luke J Prendergast[1], Kenneth Gavin[2], David Hester[3]
[1]Centre for Critical Infrastructure Research, School of Civil Engineering, University College Dublin, Belfield, Dublin 4, Éire
[2] Gavin and Doherty Geosolutions, Beech Hill Office Campus, Clonskeagh, Dublin 4, Éire
[3]School of Planning, Architecture and Civil Engineering, Queen's University Belfast, University Road, Belfast, BT7 1NN, Northern Ireland, United Kingdom
E-mail: luke.prendergast@ucd.ie, kgavin@gdgeo.com, d.hester@qub.ac.uk

ABSTRACT: Vibration-based Structural Health Monitoring (SHM) is an area of ongoing research and has received much attention from researchers in recent years. Online damage detection methods for bridges rely on placing sensors on the structure to detect anomalies in measured parameters such as acceleration, frequency or displacement among others. Changes in these parameters can be used to infer the presence of damage such as cracking in bridge beams, foundation scour etc. These methods mostly rely on using the signals arising on a bridge from ambient traffic or environmental loading. For foundation scour detection purposes, the lateral response of a bridge is of particular interest in that this has been shown to be particularly sensitive to the scour phenomenon. Vehicle-Bridge Interaction (VBI) effects can have a significant influence on the condition of output vibrations from a bridge element. In this paper, the effect of vehicle travelling velocity on the lateral response of a typical highway two-span integral bridge is investigated. In this context, the term lateral refers to the traffic direction. It is shown that depending on the velocity of the vehicle relative to the oscillatory period of the bridge it traverses, the bridge's dynamic response is either amplified or diminished by varying degrees. This phenomenon could influence the accuracy of a particular damage detection method relying on output system vibrations to infer damage.

KEY WORDS: Bridge Dynamics, Damage Detection, Vibration, SHM

1 INTRODUCTION

Structural Health Monitoring (SHM) is the art of monitoring the condition of a structure over its lifetime with a view to preventing excessive damage from accumulating. A very comprehensive overview of the topic is available in Farrar and Worden [1]. The motivation for asset owners (of bridges, in particular) for implementing technology of this nature is due to the potentially life-saving and economic benefits it can have by offsetting the cost (both in life and monetary terms) of excessive damage arising in the structure during its lifespan.

Online damage detection refers to detecting damage arising in a structure using sensors distributed on the structure. These sensors seek anomalies in the structural behavior during operation (by monitoring displacement, acceleration, frequency, mode shapes etc.). Dimarogonas [2] points out that this type of online damage detection began in the early 1970s when utility companies started looking at developing ways of identifying defects in rotating shafts while machinery was in use. To date, this is the most mature application of SHM in terms of being successful.

Vibration-based damage detection and health monitoring is an area of increased research interest in recent times [3–7]. The methods typically rely on the simple idea that damage arising in a structure will lead to changes in the structural stiffness at various locations, i.e. crack formation in a bridge beam leads to a local loss of bending stiffness. Since the modal properties of a dynamic system are inherently linked to its stiffness (and mass), damage will lead to changes in these properties.

Foundation scour is the term given to describe the process of soil erosion that can occur around bridge foundations due to adverse hydraulic action [6,8]. This is a very serious problem that is notoriously difficult to predict and detect [9]. Applying SHM techniques to scour detection has gained significant traction in recent years [5,10–16]. A common conclusion among researchers in this field is that the lateral response of a bridge sub-structural component (piles, pier) is the most sensitive to scour in terms of changes in modal properties [5,6,10,15,16]. It is therefore of interest to investigate phenomena that can affect the lateral dynamic response, or more specifically, impede the ability for a sensor located on the structure to effectively detect this response. The most practical way to excite a bridge (for vibration-based damage detection applications) is to use ambient traffic [17]. In this paper, the effect of vehicle travelling velocity as it traverses a bridge is investigated to highlight the significant effect that this can have via interaction with the bridge's own oscillatory motion (in the traffic direction). The type of bridge investigated is two-span integral bridges, due to their increasing popularity and prevalence.

2 NUMERICAL MODELLING

The issue relating to a vehicle travelling velocity across a two-span integral bridge is investigated using numerical modelling approaches. A mathematical model describing the dynamic system (the bridge) is developed in the MATLAB programming environment. Various aspects of the model are discussed in the following sub-sections. Section 2.1 briefly describes different types of integral bridges and section 2.2

describes the mathematical approach taken to model the bridge, the foundation soil and the vehicle load in this paper.

2.1 Types of Integral Bridge

Integral bridges are becoming increasingly popular as they do not require a conventional expansion joint and this can reduce maintenance costs significantly. There are four main types of integral bridge [5]: (1) Frame Abutment Type: In this type of bridge, the abutments form a portal frame with the bridge deck; (2) Bank Pad Abutment Type: In this type, an integral support exists between the bridge deck and bank pad end support; (3) Flexible Abutments: In this type, the abutments are formed as a series of piles or columns extending to the bank pad. These columns are not directly in contact with the soil but are placed in sleeves to allow better absorption of the bridge deck thermal movements; (4) Semi-Integral Abutment Type: In this type, there is an end screen wall which is integral with the bridge deck, however this wall does not directly support the bridge beams. The deck must be supported by some other mechanism. In this paper, type (3), a bridge with flexible support abutments, is modelled. A schematic of this type of bridge is shown in Figure 1.

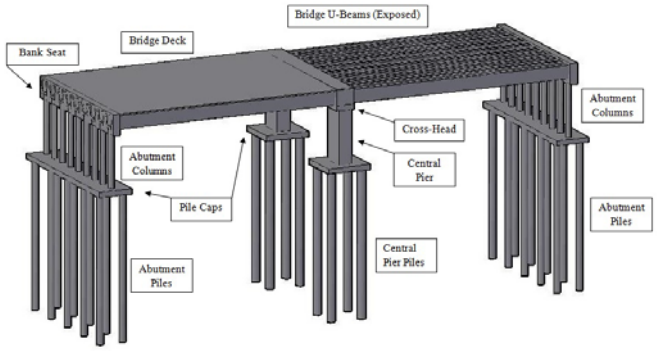

Figure 1. Schematic of Integral Bridge [5]

2.2 Mathematical Considerations

The bridge is modelled as a dynamic system. For ease of modeling, the integral bridge is treated as a 2D frame system and grouped geometric properties are used to model group behavior of the piles, abutments and piers as well as the individual deck beams. In short, lateral (into the page) and torsional behavior is omitted.

The individual bridge elements are modelled using 6-degree-of-freedom (6-DOF) Euler-Bernoulli frame elements [18], the mass $\mathbf{[M_b]}$ and stiffness $\mathbf{[K_b]}$ matrices as shown in (1). The foundation soil is modelled using a Winkler philosophy which models the continuous soil layers as discrete, mutually independent and closely spaced springs [19,20]. These spring elements have individual stiffness matrices $\mathbf{[K_{s,i}]}$ as shown in (2) and a null mass assumption.

$$\mathbf{[M_b]} = \frac{\rho AL}{420}\begin{bmatrix} 140 & 0 & 0 & 70 & 0 & 0 \\ \vdots & 156 & 22L & 0 & 54 & -13L \\ \vdots & & 4L^2 & 0 & 13L & -3L^2 \\ \vdots & & \iddots & 140 & 0 & 0 \\ \vdots & \iddots & & & 156 & -22L \\ \iddots & \cdots & \cdots & \cdots & \cdots & 4L^2 \end{bmatrix} \quad (1a)$$

$$\mathbf{[K_b]} = \begin{bmatrix} \frac{EA}{L} & 0 & 0 & -\frac{EA}{L} & 0 & 0 \\ \vdots & \frac{12EI}{L^3} & \frac{6EI}{L^2} & 0 & -\frac{12EI}{L^3} & \frac{6EI}{L^2} \\ \vdots & & \frac{4EI}{L} & 0 & -\frac{6EI}{L^2} & \frac{2EI}{L} \\ \vdots & & \iddots & \frac{EA}{L} & 0 & 0 \\ \vdots & \iddots & & & \frac{12EI}{L^3} & -\frac{6EI}{L^2} \\ \iddots & \cdots & \cdots & \cdots & \cdots & \frac{4EI}{L} \end{bmatrix} \quad (1b)$$

$$\mathbf{[K_{s,i}]} = k_{s,i}\begin{bmatrix} 1 & -1 \\ -1 & 1 \end{bmatrix}, \quad k_{s,i} \geq 0 \quad (2)$$

To model the bridge, knowledge of E (Young's modulus), I (moment of inertia), A (cross-sectional area) for each element is required as well as span lengths, column lengths etc. Standard properties are adopted to model the integral bridge in this paper and these properties are available in [5,6]. In summary, a two-span concrete bridge with each span being 25 m in length is modelled. A schematic showing the main model dimensions is produced in Figure 2. This figure also shows an inset of the individual bridge element degrees of freedom.

To model the foundation soil, the approach described by Prendergast et al. [5,11,21] is used. This approach considers each soil spring as a linear-elastic element (strain-independent $\boldsymbol{k_{s,i}}$) and uses small-strain soil stiffness parameters (G_0, E_0) to characterize the response. The approach was developed based on experimental work carried out to develop correlations between measurable geotechnical site data (Cone Penetration Tests, Multi-Channel Analysis of Surface Waves (MASW) [22]) and geotechnical stiffness parameters [10,23]. These approaches allow for soil spring stiffnesses to be specified that are capable of modeling a normally-consolidated loose, medium-dense or dense sand deposit. In this paper, the bridge is assumed to be founded in loose sand.

From the individual structural matrices shown previously, global mass $\mathbf{[M_G]}$ and stiffness $\mathbf{[K_G]}$ matrices are assembled for the full structure according to the procedure in Kwon & Bang [18]. The dynamic response of the bridge structure can be obtained by solving the second-order matrix differential equation shown in (3) using a numerical integration scheme. In this paper, the Wilson-Θ integration scheme is used [24].

$$\mathbf{[M_G]}\begin{Bmatrix} \ddot{\mathbf{x}}_1(\mathbf{t}) \\ \ddot{\mathbf{x}}_2(\mathbf{t}) \\ \vdots \\ \ddot{\mathbf{x}}_N(\mathbf{t}) \end{Bmatrix} + \mathbf{[C_G]}\begin{Bmatrix} \dot{\mathbf{x}}_1(\mathbf{t}) \\ \dot{\mathbf{x}}_2(\mathbf{t}) \\ \vdots \\ \dot{\mathbf{x}}_N(\mathbf{t}) \end{Bmatrix} + \mathbf{[K_G]}\begin{Bmatrix} \mathbf{x}_1(\mathbf{t}) \\ \mathbf{x}_2(\mathbf{t}) \\ \vdots \\ \mathbf{x}_N(\mathbf{t}) \end{Bmatrix} = \begin{Bmatrix} \mathbf{F}_1(\mathbf{t}) \\ \mathbf{F}_2(\mathbf{t}) \\ \vdots \\ \mathbf{F}_N(\mathbf{t}) \end{Bmatrix} \quad (3)$$

where $\mathbf{[M_G]}$, $\mathbf{[C_G]}$ and $\mathbf{[K_G]}$ are the (N x N) global mass, damping and stiffness matrices for the model respectively and N is the total number of degrees of freedom in the system.

$\{\mathbf{x}(\mathbf{t})\}$, $\{\dot{\mathbf{x}}(\mathbf{t})\}$ and $\{\ddot{\mathbf{x}}(\mathbf{t})\}$ describe the displacement, velocity and acceleration of every degree of freedom for each time step in the analysis and $\{\mathbf{F}(\mathbf{t})\}$ describes the external forces acting on each of the degrees of freedom for a given time step. These external forces are determined by apportioning the vehicle load as forces and moments on adjacent bridge nodes as the load traverses the bridge, using Hermitian shape functions (interpolation functions). The damping matrix **[C_G]** is determined assuming a Rayleigh damping approach [25] and a damping ratio ($\xi_1 = \xi_2 = \xi$) of 2% is assumed .

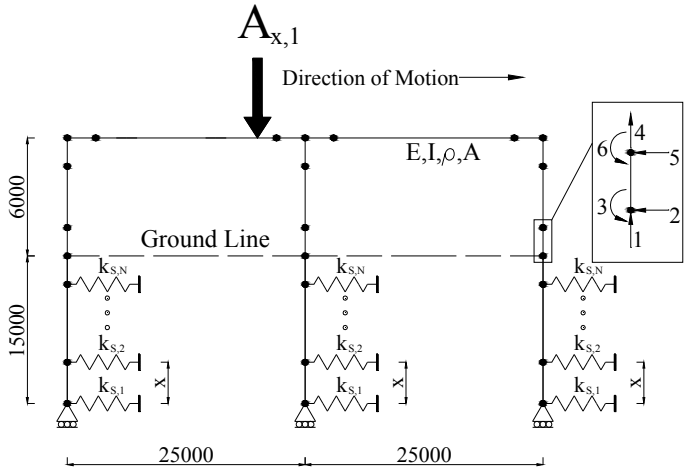

Figure 2. Model Schematic and Dimensional Data (mm)

3 VELOCITY EFFECTS

In this section, the interaction effects between a vehicle's travelling velocity over the bridge and the resulting impact on the bridge's own oscillatory motion (in the traffic direction) is investigated. Section 3.1 presents an analysis of the mode shape of the bridge pertaining to lateral sway motion and section 3.2 investigates the effect of a single vehicle load traversing the bridge.

3.1 Global mode shape of bridge

In order to extract the un-damped modal frequencies and mode shapes from the numerical model, it is necessary to conduct an eigenvalue analysis on the system matrix **[D]**, specified as shown in (4).

$$[\mathbf{D}] = [\mathbf{M_G}]^{-1}[\mathbf{K_G}] \tag{4}$$

An eigenvalue analysis is conducted on **[D]** using MATLAB's in-built eigenvalue functionality. Extracting the system eigenvalues and eigenvectors corresponds to the un-damped frequencies and mode shapes of the model.

The fundamental mode shape of the integral bridge is a global lateral sway mode (in the traffic direction). For the given bridge properties assumed [5], the frequency of the fundamental mode is 1.5643 Hz with a corresponding period (*T*) of 0.639 seconds. The bridge modal shape at four vibration stages corresponding to 0.25 x *T*, 0.5 x *T*, 0.75 x T, and 1 x *T* is shown in Figure 3.

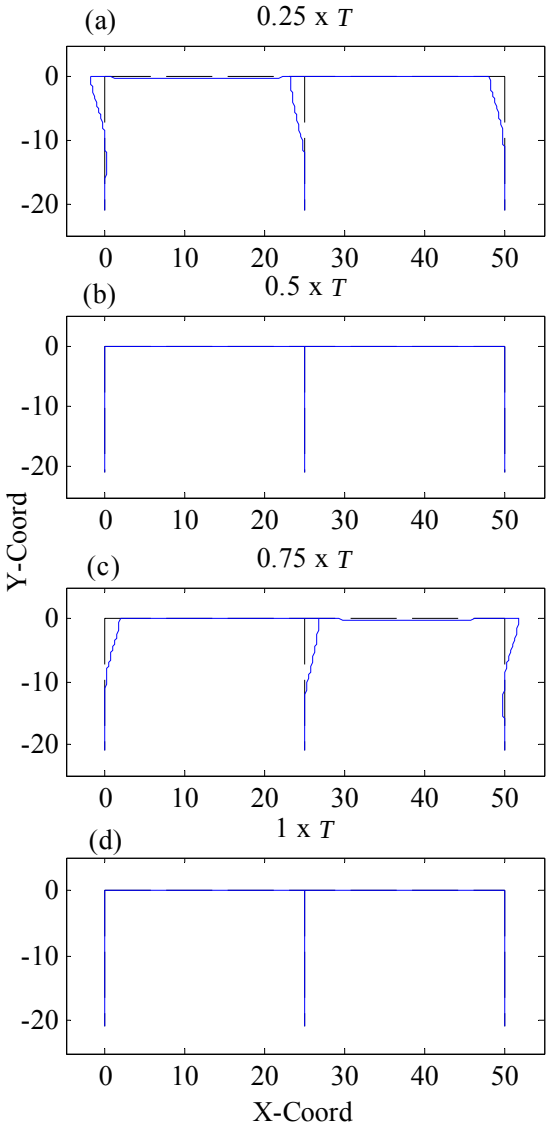

Figure 3. Four stages of first vibration mode – global sway

Figure 3 provides a pictorial view of the displaced shape of the given mode at a particular stage of vibration over one cycle. The time it takes for the given shape to arise and the direction of motion is displayed in Table 1.

Table 1. Bridge motion – direction and arrival times.

Fig 3 Image Ref	Arrival Time (s)	Motion Direction
(a)	0.25 x 0.639 = 0.16s	Stationary (will move right)
(b)	0.5 x 0.639 = 0.32s	Swaying to right
(c)	0.75 x 0.639 = 0.4795s	Stationary (will move left)
(d)	1 x 0.639 = 0.639s	Swaying to left

Interaction effects between the bridge's dynamic motion and the rate of load traversing are investigated in the next section.

3.2 *Single traversing load*

While the bridge undergoes global sway at the first natural frequency (see Figure 3), it first sways to the left (say) with span 1 deflecting downward, then sways right with span 2 deflecting downward. If we consider a single load traversing the bridge while it undergoes motion at its own natural frequency, the rate at which the load traverses will interact with the amplitude of the bridge's lateral motion. This will lead to differences in the magnitude of the free vibration response after the load (vehicle) has left the bridge. As the lateral bridge motion is the parameter of interest, a typical lateral displacement and acceleration response measured at the pier top due to a single load traversing is shown in Figure 4. For this analysis, the load of V = 100 kN traverses the bridge at 25 m/s and the signal contains 10 seconds of free vibration after the load departs.

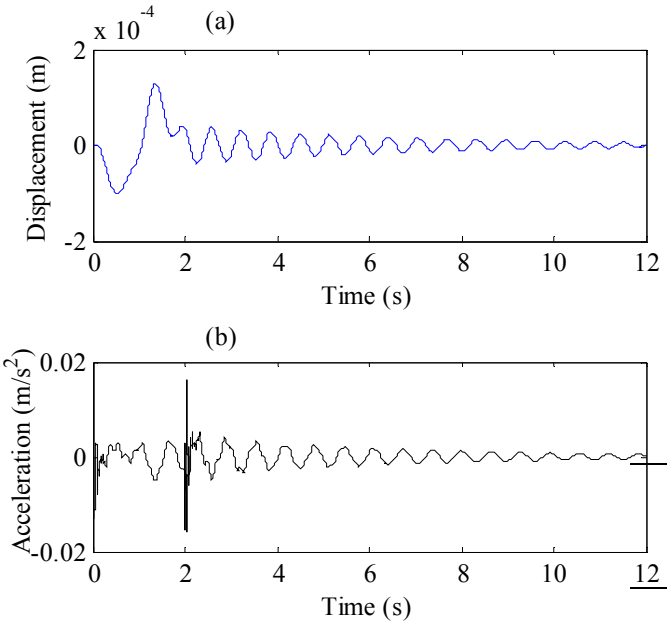

Figure 4. Pier top signals for load traversing at 25 m/s with 10 sec free vibration. (a) Lateral displacement. (b) Lateral acceleration.

The signals in Figure 4 are quite typical. The individual peaks as the load enters and leaves the bridge are evident in the acceleration plot in part (b). Once the load leaves the bridge, a logarithmic decay is evident in the free vibration of both displacement and acceleration. It is postulated in this paper that the rate at which the load traverses the bridge will affect the amplitude of the response signals due to interaction effects. More specifically, maximum amplification of the response should occur if the load traverses the first span in the time it takes for the bridge to undergo one half of its vibration cycle (i.e. reaching the pier when the bridge is in condition (b) of Figure 3). This means that the load will be on the left span when it naturally deflects downwards and on the right span when this naturally deflects downwards due to the bridge's periodic motion, thus amplifying this response. The opposite situation (maximum diminishing of signal) should occur if the load traverses span 1 in the time it takes for the bridge to undergo a full vibration cycle (i.e. condition (d) in Figure 3). This is because in this case the load while on the left span for the first half of the vibration cycle will still be on the left span during the second half, where it will act against the bridge's natural motion, then it will pass onto the right span while the bridge is naturally pulling left for the first half of the next cycle, once more impeding the motion before finally working with the bridge for the second half of its second cycle.

To investigate this, an analysis is conducted herein. For the analysis in this paper, only the free vibration signal after the vehicle (load) leaves the bridge is produced. This is because as the load is on the bridge, it is more difficult to compare different responses due to the different times associated with the load leaving the bridge making direct comparisons difficult. A single load traverses the bridge with a velocity (v_s) such that it crosses the first bridge span (25 m) in a time that is a given ratio of the bridge's natural period. The ratios chosen are 0.25, 0.5, 0.75, 1, 1.25, 1.5 1.75 and 2 times the bridge's natural period (T). The results of this analysis should confirm that a load traversing the bridge span 1 in a time that equates to half of the bridge's natural period is the most beneficial in terms of signal amplification (free vibration) while a load traversing the span 1 in a time equating to the full bridge period will impede the vibration the most. Establishing the effect at multiples of the bridge period (i.e. ratios > 1) is also undertaken to observe if the effect is any different and also to see how the system reacts with more realistic loading velocities. Table 2 outlines the crossing times and required velocities for the analysis. Note: for the analysis with ratios < 1 for crossing velocities, the vehicle (load) speeds are unrealistically high.

Table 2. Load velocities to traverse span 1.

Span (m)	T (s)	Time to cross Span 1 T_v (s)	Ratio T_v/T	Load v_s (m/s)
25	0.639	0.16	0.25	156.43
25	0.639	0.32	0.5	78.22
25	0.639	0.4794	0.75	52.14
25	0.639	0.639	1	39.11
25	0.639	0.799	1.25	31.29
25	0.639	0.959	1.5	26.07
25	0.639	1.118	1.75	22.36
25	0.639	1.278	2	19.56

The results for the analysis are shown in Figure 5 and 6. Figure 5(a) shows the lateral pier top displacement responses in free vibration for velocity ratios ≤ 1. Figure 5(b) shows the lateral pier top acceleration responses in free vibration for velocity ratios ≤ 1. Five seconds of free vibration is analysed. In Figure 5 it is evident that the maximum amplification of the free vibration response signals occurs for a load traversing the first span in the time it takes the bridge to undergo 0.5 times its vibration cycle. It is also shown that the lowest amplification of the signal occurs when the load traverses the first span in the time it takes the bridge to undergo a full cycle. The other ratios give intermediate results and the results are the same for both displacement and acceleration. This is sensible (and expected) as it indicates that when the load is completely in phase with the bridge motion (i.e. pushing down

on span 1 as it naturally deflects downwards due to periodic motion, then moving to span 2 as this naturally deflects downwards) we achieve maximum amplification. When the load acts to resist the bridge's own oscillatory motion, we achieve the lowest amplification.

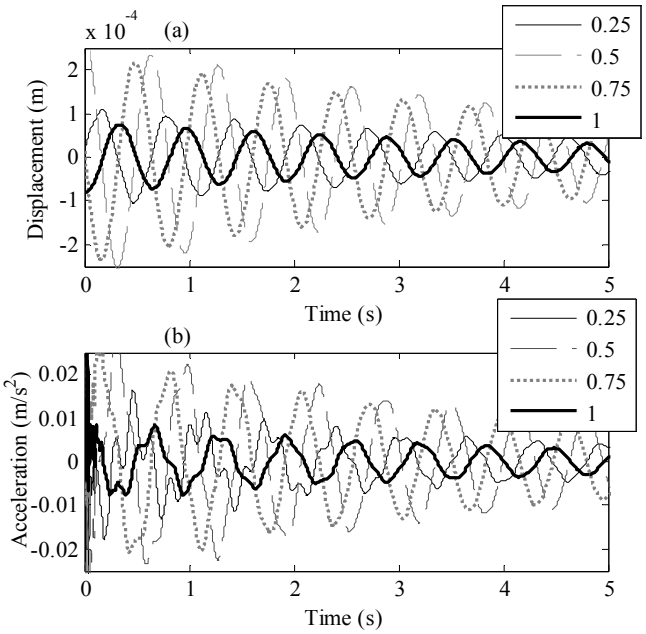

Figure 5. Lateral pier top signals for load traversing span 1 in specified ratio (0 to 1) of bridge period. (a) Displacement. (b) Acceleration.

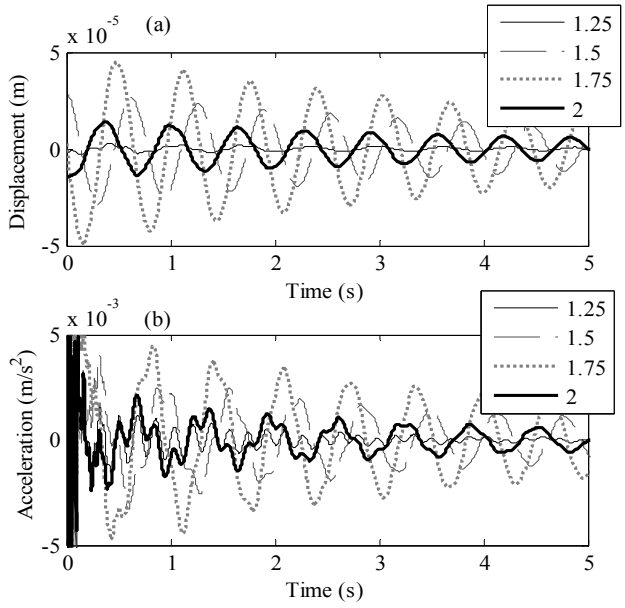

Figure 6. Lateral pier top signals for load traversing span 1 in specified ratio (1 to 2) of bridge period. (a) Displacement. (b) Acceleration.

Figure 6 shows the results for the load traversing span 1 in a time that is multiples of the bridge's natural period. The amplitude results in this case are almost an order of magnitude less pronounced (to be expected as there is an element of the load acting against the bridge movement for every case). The results for Figure 6 indicate a different outcome than those in Figure 5. The maximum signal amplification occurs when the load reaches the end of span 1 in a time that is 1.75 times the bridge's period as opposed to 1.5 times which might have been expected from the first set of results. Also the lowest amplification occurs for the load traversing span 1 in 1.25 times the bridge period as opposed to 2 times, as might have been expected. The amplitude of the free vibration is a function of the bridge displacement, velocity and acceleration at the point when the load leaves the bridge and this can have a significant effect on the amplitude of the signal in free vibration. The results are less intuitive than when the load traverses in a specified ratio less than 1 of the bridge period as in this case it is easy to see when the load will act to impede the bridge motion. For ratios greater than 1, there is a trade-off effect in place as at some stage during the loading, the load will always be 'working against' the bridge motion to some degree. These results highlight the complicated interaction process at play in this problem and moreover show that using vehicle-induced vibration signals for bridge damage detection could potentially lead to issues with time-domain based SHM techniques.

4 CONCLUSION

Vibration-based Structural Health Monitoring is a growing research area. In this paper we describe the application of the approach to investigate reliable methods to detect damage arising in bridge structures using dynamic response measurements. For scour detection using vibration-based methods, the lateral response of a bridge sub-structural element has been shown to be most sensitive to scour. Obtaining dynamic signals from a bridge is mostly undertaken by monitoring its response to ambient traffic loading. Therefore, it is of interest to study potential effects that could arise from the interaction between the rate of loading a two-span integral bridge and the measured response.

In this paper, vehicle velocity effects were investigated in terms of how they can amplify or diminish the dynamic response of a bridge. The results show that the response magnitude in free vibration can vary significantly depending on how the load interacts with the bridge in terms of its own oscillatory motion. The results in many cases may not be intuitive and this study aims to highlight potential disparities that can arise.

This phenomenon could become an issue for time-domain related SHM techniques, as a diminished signal magnitude could become absorbed into the noise band of a standard sensor for example. Signal clarity can be a serious issue for many of these methodologies.

ACKNOWLEDGMENTS

The authors wish to acknowledge the support of the European Union H2020 project DESTination RAIL (Project No. 636285) and the Geological Survey of Ireland (GSI) Short-Call 2015 (Project No. 2015-SC-035) .

REFERENCES

[1] Farrar CR, Worden K. An introduction to structural health monitoring. Philos Trans A Math Phys Eng Sci 2007;365:303–15.

[2] Dimarogonas AD. Vibration of cracked structures: A state of the art review. Eng Fract Mech 1996;55:831–57.

[3] Hester D, González A. A wavelet-based damage detection algorithm based on bridge acceleration response to a vehicle. Mech Syst Signal Process 2012;28:145–66.
[4] González A, Hester D. An investigation into the acceleration response of a damaged beam-type structure to a moving force. J Sound Vib 2013;332:3201–17.
[5] Prendergast LJ, Hester D, Gavin K. Development of a Vehicle-Bridge-Soil Dynamic Interaction Model for Scour Damage Modelling. Shock Vib 2016;2016.
[6] Prendergast LJ, Hester D, Gavin K. Determining the presence of scour around bridge foundations using vehicle-induced vibrations. J Bridg Eng 2016;In Press.
[7] Prendergast LJ, Gavin K, Reale C. Sensitivity studies on scour detection using vibration-based systems. Transp Res Procedia 2016;14C:3982–9.
[8] Hamill L. Bridge Hydraulics. London: E.& F.N. Spon; 1999.
[9] Prendergast LJ, Gavin K. A review of bridge scour monitoring techniques. J Rock Mech Geotech Eng 2014;6:138–49.
[10] Prendergast LJ, Hester D, Gavin K, O'Sullivan JJ. An investigation of the changes in the natural frequency of a pile affected by scour. J Sound Vib 2013;332:6685–702.
[11] Prendergast LJ, Gavin K, Doherty P. An investigation into the effect of scour on the natural frequency of an offshore wind turbine. Ocean Eng 2015;101:1–11.
[12] Ju SH. Determination of scoured bridge natural frequencies with soil–structure interaction. Soil Dyn Earthq Eng 2013;55:247–54.
[13] Foti S, Sabia D. Influence of Foundation Scour on the Dynamic Response of an Existing Bridge. J Bridg Eng 2011;16:295–304.
[14] Klinga J V., Alipour A. Assessment of structural integrity of bridges under extreme scour conditions. Eng Struct 2015;82:55–71.
[15] Briaud JL, Hurlebaus S, Chang K, Yao C, Sharma H, Yu O, et al. Realtime monitoring of bridge scour using remote monitoring technology. vol. 7. Austin, TX: 2011.
[16] Elsaid A, Seracino R. Rapid assessment of foundation scour using the dynamic features of bridge superstructure. Constr Build Mater 2014;50:42–9.
[17] Farrar CR, Duffey TA, Cornwell PJ, Doebling SW. Excitation methods for bridge structures. Proc. 17th Int. Modal Anal. Conf. Kissimmee, vol. 7, Kissimmee, FL: 1999.
[18] Kwon YW, Bang H. The Finite Element Method using MATLAB. Boca Raton, FL: CRC Press, Inc.; 2000.
[19] Dutta SC, Roy R. A critical review on idealization and modeling for interaction among soil–foundation–structure system. Comput Struct 2002;80:1579–94.
[20] Winkler E. Theory of elasticity and strength. Dominicus Prague: 1867.
[21] Prendergast LJ, Gavin K. A comparison of initial stiffness formulations for small-strain soil – pile dynamic Winkler modelling. Soil Dyn Earthq Eng 2016;81:27–41.
[22] Donohue S, Long M, Gavin K, O'Connor P. Shear Wave Stiffness of Irish Glacial Till. Int. Conf. Site Characterisation I, Porto, Portugal: 2004, p. 459–66.
[23] Prendergast LJ, Gavin K, Igoe D. Dynamic soil-structure interaction modeling using stiffness derived from in-situ Cone Penetration Tests. 3rd Int. Symp. Cone Penetration Test., Las Vegas, NV: 2014.
[24] Tedesco JW, McDougal WG, Allen Ross C. Structural Dynamics: Theory and Applications. 1999.
[25] Yang Y, Yau J, Wu Y. Vehicle-bridge interaction dynamics. 2004.